Structural and Dielectric Properties of BaCexTi1-xO3 Ceramics

Deepak Kumar, Chetan Thakur
Student
Galgotias University

Abstract - Lead-free $BaTiO_3$-based materials is the replacement of lead-based materials for various dielectric applications. These materials having excellent piezoelectric, pyroelectric and ferroelectric properties in comparison of lead-based counterparts. In this article, the role of Cerium dopant on microstructural and dielectric performance of $BaCe_xTi_{1-x}O_3$ (BCT) ceramics with compositions x=0, 0.1, 0.12 and 0.15 is investigated in detail. A diffuse phase transition is typical for all the Ce doped compositions, with a substantial reduction of the Curie temperature towards room temperature. The performance of $BaCe_{0.15}Ti_{0.85}O_3$ was good with respect to other samples.

Keywords - Ferroelectric, Dielectrics and Piezoelectric

1. Introduction

Ferroelectric oxide ceramics are used in a very broad range of functional ceramics and form the materials base for the majority of electronic applications like various types of sensors, actuators, buzzers, medical ultrasonic transducers and other electronic devices. [1-3]. Interest in lead-free ferroelectric ceramics has sparkled over the period of time owing to the need to find a suitable replacement of its lead based counterparts namely lead zirconate titanate ($Pb(Zr,Ti)O_3$, PZT) which contains ~60 wt.% of toxic lead[4-6]. In this context, as their replacement, these three well known ferroelectrics based on $BaTiO_3$, $KNbO_3$, and $Na_{1/2}Bi_{1/2}TiO_3$ in pure and modified forms have been explored with renewed interest in the last decade. A perusal of literature suggests that Zr [6-7], Sn [7,8] and Hf [7,9] substitutions in $BaTiO_3$ proposes interesting opportunity to chemically tune the orthorhombic-tetragonal and rhombohedral-orthorhombic phase transitions near to room temperature for enhanced piezoelectric properties. In another study by Yao et.al, a giant piezoelectric coefficient (d_{33}) of 697 pC/N has been found in $BaTiO_3$-11$BaSnO_3$ which is highest reported value till date [10]. As part of the on-going research on lead-free ceramics, it is of prime motive to develop further the various types of cations whose substitution at the Ba and/or Ti sites could enhance the performance of base composition for many dielectric applications, similar to that of Zr, Hf, and Sn. All these findings incited worldwide exploration on $BaTiO_3$-based materials for replacement of lead-based materials for various dielectric applications. One of the captivating features of $BaTiO_3$ ceramics is that by forming solid solutions with some of the rare earth ions like Ce [11] and Y [12], a relaxor behaviour with enhanced dielectric, piezoelectric and pyroelectric performance can be induced. Among the $BaTiO_3$ based ferroelectrics, $BaTiO_3$ doped with Ce garnered researchers scrutiny both due to application and fundamental interests [13-15]. The dopant ion Ce can enter into $BaTiO_3$lattice as Ce^{3+} or Ce^{4+}. The ionic radii of Ce^{3+} is in close proximity to that of Ba^{2+} ion which makes Ce^{3+} to occupy Ba site[12]. Ce^{4+} having an ionic radius in close proximity with that of Ti^{4+} will substitute Ti sites [14]. Further it is the fact that Ce^{4+} ion being more stable than Ce^{3+} ion will occupy Ti site. Therefore, it is of prime importance to study the site occupancy of Ce in $BaTiO_3$ perovskite lattice. In this context, few studies reveal the substitution of Ce ions can take place at both sites (A and B) in the $BaTiO_3$ perovskite unit cell when concentration of Ce<8% which can result in completely different characteristics [16]. Curecheriu *et.al.* studied the site occupancy for Ce>=0.1 and the peculiar features observed by him indicated the B site occupancy of Ce [17]. This system has not been investigated in detail so far in literature. For instance, Ang*et.al*. have reported the electric field induced strain behaviour for some cerium-doped $BaTiO_3$ compositions [16,18]. Makovec*et.al.* [14] proposed a detailed phase diagram of $CeO–BaO–TiO_2$, while more recently Brajesh*et. al.* [19] discussed about the relationship between the ferroelectric instability and large piezoelectric coefficient in Ce-BT ceramics with small cerium amount (y<0.12). Recently, the dielectric and ferroelectric P-E hysteresis characteristics were investigated by Curecheriu *et.al.* for $BaCe_yTi_{1-y}O_3$ ceramics with y=0.1, 0.2 and 0.3 and explored these materials for application as tunable capacitors [15]. In view of this, we limited ourselves to examine the structural, dielectric and ferroelectric behaviors of few Ce doped $BaTiO_3$ [$BaCe_xTi_{1-x}O_3$ (x=0, 0.1, 0.12, 0.15)] in the present work.

2. Experimental

The ceramics of composition $BaCe_xTi_{1-x}O_3$ (x=0, 0.1, 0.12 and 0.15) were synthesised using solid state reaction route. High purity analytical reagent grade powders of barium carbonate [$BaCO_3$,(99% pure)], Titanium dioxide [TiO_2,(99% pure)] and rare earth oxide Ceric oxide [CeO_2,(99.99% pure)] were used as the starting precursors. These starting materials were weighed according to their stoichiometric ratio and ball milled for 10 h in acetone as the wetting agent to have physical homogeneity. The mixture after drying was subjected to calcination at 1000^{o}C for 4h. Following calcination, the resultant mixture was pressed to form a disc shaped pellets having a diameter of 12 mm and a thickness of 1 mm after mixing 2% by weight

polyvinylalcohol (PVA) which acts as a binder lubricant. The green samples were sintered at 1500°C for 9 hours. Afterwards, the density of the samples was measured employing Archimedes principle.
The sintered ceramics were characterized by X-ray diffraction (XRD) (Rigaku Smart Lab, Japan).Scanning electron microscopy (SEM) (FEI SEM NOVA Nanosem 450, Hillsboro, OR) was used to study the samples surface morphology.
For the electrical measurements, silver electrodes were used on the polished surface of the ceramic samples. The polarization-electric field (P-E) hysteresis loops were recorded at various temperatures using a modified Sawyer Tower circuit (Marine India). The dielectric constant and loss were determined using impedance analyzer (Agilent E4990A, Agilent Technologies Inc., Santa Clara, CA).

3. Results and Discussion

Fig. 1 shows the XRD patterns of the $BaCe_xTi_{1-x}O_3$ceramics for various Ce content (x=0, 0.1, 0.12, 0.15) sintered at 1500°C/9 hrs. The lack of any secondary peaks indicates that the solid state reaction has occurred in the specified sintering conditions. The structural analysis evidences that the limit of solid solubility of Ce^{4+} ions to Ti ions in $BaTiO_3$ lattice is around x=0.3 as reported by Anget.al. [18]. The diffraction peaks of the undoped ceramic correspond well to T-symmetry (PDF#05-0626) [21]. We observe that the peak intensity splits into two {(002), (200)} at angles ranging from 44°-46° as evident from fig.1 which indicates that the ceramic also possess an O-phase corresponding to (PDF#81-2200) [21]. Also, it is noticed that three peaks at 56° in x=0 sample which corresponds well to the standard card (PDF#81-2200), which further confirms the existence of O-phase in pristine $BaTiO_3$ [21].However, with the introduction of Ce into the lattice of $BaTiO_3$, the diffraction peaks around 44°-46° merge into a single peak, suggesting that the host phase undergoes an obvious phase transition. These three peaks at 56° also merge into a single peak for all Ce added samples under study. Apart from the structural phase transition, we also noticed a gradual shift of diffraction peak towards lower angle with increasing x content. It could be due to the replacement of larger ion Ce^{4+} (r=0.87 Å) for Ti^{4+} (r=0.6507Å) at the B site of perovskite structure [17]. Hence, in the present work, XRD is limited only to confirm the phase as the main focus of this article is to explore these materials for specific properties as discussed in subsequent sections. However, we believe a detailed discussion on XRD analysis is required to understand the structural evolution.
The scanning electron microscopy (SEM) images of all the investigated compositions exhibit well interconnected grains and without major voids or anomaly, having a bimodal grain size distribution (larger grains coexist with smaller grains) as shown in fig.2. With Ce addition, a further increase of larger grains on the expense of smaller grains takes place which is in agreement with the work reported by Curecheriu et.al. [15]. Further, the densities of $BaCe_xTi_{1-x}O_3$ sintered ceramics were found employing Archimedes principle and the relative densities were all >93% for all compositions.
Figure 3 shows the P-E hysteresis loops of Ce doped $BaTiO_3$ ceramics at constant electric field of 24kV/cm and at room temperature. All the investigated materials show well-saturated loops indicative of classical ferroelectric-like loops. The remnant polarization (P_r) and coercive field (E_c) values are ~7 μC/cm^2 and ~3.5 kV/cm, respectively, for base composition x=0. Hysteresis loops become thinner and thinner as the content of Ce increases accompanied by a fast drop of E_c. Such a low value of E_c suggests that the compositions are soft with respect to electric field.
Fig. 4 shows the temperature dependence of dielectric constant and dielectric loss (tan δ) for all BCT ceramics measured at various frequencies. It can be deducted from fig.5 that Curie temperature decreases when the content of Ce increases. One of the intriguing characteristics of normal ferroelectric ceramic is that they are suspected to obey Curie–Weiss law under the application of high temperatures (above Curie) and they follow Eq.1: [22].

$$\varepsilon = \frac{C}{T - T_{CW}} \quad (1)$$

Where C stands for Curie –Weiss constant, T_{CW} is the Curie–Weiss temperature and ε is dielectric constant. This study will be helpful to further analyse the phase transition behaviour. The Curie–Weiss constant reflects the nature of the ferroelectric transition. As C is of the order of 10^5°C, the high temperature paraelectric phase is driven by a displacive transition, and with 10^3 °C order, the transition will be more likely to be order-disorder [22, 25-27]. In BCT system, all C are of the order of 10^5 °C, suggesting that the high temperature paraelectric phase is driven by a displacive transition. In order to make the value of T_{CW} certain, the inverse of dielectric constant ($1/\varepsilon$) versus temperature (T) at 1 MHz is plotted as portrayed in fig. 5 (a)-(d). It is found that the dielectric permittivity of pure BT ceramics well obeys the Curie–Weiss law above the Curie temperature. However, the dielectric permittivity of BCT ceramics obviously deviates from the Curie–Weiss law when the content of Ce increases. This deviation from the Curie–Weiss law can be mathematically expressed as follows: [22, 23, 29].

$$\Delta T_m = T_B - T_m \quad (2)$$

Where T_m stands for temperature corresponding to peak of dielectric and T_B stands for the temperature from which the dielectric permittivity starts to follow the Curie–Weiss law. This temperature is referred to as Burns' temperature. The temperature associated with peak of dielectric (T_m) is 395 K (pure BT) which can be decreased to 330 K upon addition of 15% Ce content. On similar grounds, T_{CW} also decreases from 389 K to 341 K. It can be said that the phase transition temperature range (around T_m) becomes lower and broadening increases with increase in Ce content which can be credited to phase change: from ferroelectric to diffuse. Hence, to study the phase transition behaviour of BCT specimens, a diffuseness parameter is estimated using modified Curie–Weiss relationship. Modified Curie–Weiss law is explained using the dielectric behaviour of complex ferroelectrics with diffuse phase transition, which can be expressed as shown in Eq.3. : [24].

$$\frac{1}{\varepsilon} - \frac{1}{\varepsilon_m} = \frac{(T - T_m)^\gamma}{C} \quad (3)$$

Where C' is assumed to be constant, ε_m is dielectric maximum and γ is the diffusion coefficient. The symbols ε and T_m have their usual meaning as described above. Generally, the value of γ lies between 1 (conventional ferroelectric) and 2 (relaxor ferroelectric): [22, 23, 28]. In order to further confirm the effect of Ce content on the diffuse phase transition behaviour of the

investigated chemical composition ceramics, $ln(\frac{1}{\varepsilon}-\frac{1}{\varepsilon_m})$ is plotted against $\ln(T-T_m)$ at frequency 1 MHz as shown in the insets of fig. 5 (for x=0.12 and 0.15). It is imperative to note here that a linear relationship can be seen for all specimens. γ value is found from the slope of the fitting curves. It is found that the γ value increases from 1.26 to 1.89 with increasing x value. Additionally, the degree of diffusivity for phase transition can be formulated in terms of an empirical parameter $\Delta T_{diffuse}$ as shown by Eq.4: [24].

$$\Delta T_{diffuse} = T_{0.9\varepsilon_m} - T_{\varepsilon_m} \quad (4)$$

Where $T_{0.9\varepsilon_m}$ represents temperature corresponding to 90% of maximum dielectric constant (ε_m) at 1 MHz. It clearly manifests that diffusivity increases with Ce content. However, further research is warranted to clarify the nature of these phase transitions.

4. Conclusions

Systematic investigation of structural and dielectric performance of Ce substituted $BaTiO_3$ [$BaCe_xTi_{1-x}O_3$ (BCT)] ceramics with compositions x=0, 0.1, 0.12 and 0.15 was investigated in detail. Addition of Cerium into the lattice of $BaTiO_3$ resulted in increase in lattice constants. The Ce substitution diffused the phase transition of $BaTiO_3$ and resulted in decrease of Curie temperature which is confirmed from the dielectric measurements in $BaCe_{0.15}Ti_{0.85}O_3$. Degree of diffusivity was found to increase from 1.26 to 1.89 for x=0.15. Further d_{33} was found to be larger for x=0.1 sample which could be advantageous for many piezoelectric applications.

References

[1] Jungang Hou, Rahul Vaish, Yuanfang Qu, Dalibor Krsmanovic, K. B. R. Varma and R. V.Kumar, "Dielectric and pyroelectric properties of $Bi_4Ti_{2.98}Nb_{0.01}Ta_{0.01}O_{12}$ ceramics," *Mater. Chem. Phys.* **121**, 32 (2010).

[2] D. Sharma, S. Patel, A.Singh, R. Vaish, "Enhanced thermal energy conversion and dynamic hysteresis behavior of Sr-added $Ba_{0.85}Ca_{0.15}Ti_{0.9}Zr_{0.1}O_3$ (BCT-BZT) ferroelectric ceramics"*J. Materiomics.* **2(1)**, 75 (2015).

[3] S. Patel, K.S. Srikanth and R. Vaish, "Effect of sintering parameters on the dynamic hysteresis scaling behavior of $Ba_{0.85}Sr_{0.15}Zr_{0.1}Ti_{0.9}O_3$ ceramics" *Integrated Ferroelectrics.* **176,** 95 (2015).

[4] M.Sharma, A.Chauhan, V.S.Chauhan and R. Vaish, "Pyroelectric Materials for Solar Energy Harvesting: A Comparative Study" *Smart Materials and Structures* **24** (10), 105013 (2015).

[5] Manish Vaish and R. Vaish, "An experimental study on thermal energy harvesting using $Ca_{0.15}(Sr_{0.5}Ba_{0.5})_{0.85}Nb_2O_5$ pyroelectric ceramics" *Ferroelectrics Letters Section.* **43**(1), 52(2015).

[6] Z. Yu, C. Ang, R. Guo and A. Bhalla, " Piezoelectric and strain properties of Ba(Ti1−xZrx)O3Ba(Ti1−xZrx)O3 ceramics ", *J. Appl. Phys.*, **92**, 1489-1493(2002).

[7] A. K. Kalyani, K. Brajesh, A. Senyshyn and R. Ranjan," Orthorhombic-tetragonal phase coexistence and enhanced piezo-response at room temperature in Zr, Sn, and Hf modified $BaTiO_3$ ", *Appl. Phys. Lett.*,**104**, 252906 (2014).

[8] N. Yasuda, H. Ohwa and S. Asano," Dielectric Properties and Phase Transitions of $Ba(Ti_{1-x}Sn_x)O_3$Solid Solution", *J. Appl. Phys.*,**35**, 5099 (1996).

[9] Y. Avrahami and H. Tuller, " Improved electromechanical response in rhombohedral BaTiO 3 ", *J. Electroceram.*,**13**, 463-469(2004).

[10] S. K. Upadhyay, V. R. Reddy, P. Bag, R. Rawat, S. Gupta and A. Gupta," Electro-caloric effect in lead-free Sn doped BaTiO3 ceramics at room temperature and low applied fields ", *Appl. Phys. Lett.*,**105**, 112907 (2014).

[11] Z. Jing, C. Ang, Z. Yu, P. Vilarinho and J. Baptista," Dielectric properties of Ba (Ti 1− y Y y) O 3 ceramics ", *J. Appl. Phys.*, **84**, 983-986 (1998).

[12] F. Han, Y. Bai, L.-J. Qiao and D. Guo," Large electrocaloric strength and broad electrocaloric temperature span in lead-free $Ba_{0.85}Ca_{0.15}Ti_{1x}Hf_xO_3$ ceramics ", *J. Mater. Chem. C*, **4**, 1842-1849 (2016).

[13] Y. Park and Y. Kim," The dielectric temperature characteristic of additives modified barium titanate having core-shell structured ceramics ", *J. Mater. Res.*, **10**, 2770-2776 (1995).

[14] D. Makovec, Z. Samardžija and D. Kolar," Solid Solubility of Cerium in $BaTiO_3$", *J. Solid State Chem.*, **123**, 30-38 (1996).

[15] L. Curecheriu, C. Ciomaga, V. Musteata, G. Canu, V. Buscaglia and L. Mitoseriu," Diffuse phase transition and high electric field properties of $BaCe_yTi_{1-y}O_3$ relaxor ferroelectric ceramics", *Ceram. Int.*, **42**, 11085-11092 (2016).

[16] C. Ang, Z. Yu and Z. Jing," Impurity-induced ferroelectric relaxor behavior in quantum paraelectric SrTiO3 and ferroelectric BaTiO3", *Phys. Rev. B*, **61**, 957 (2000).

[17] L. P. Curecheriu, M. Deluca, Z. V. Mocanu, M. V. Pop, V. Nica, N. Horchidan, M. T. Buscaglia, V. Buscaglia, M. van Bael and A. Hardy," Investigation of the ferroelectric–relaxor crossover in Ce-doped $BaTiO_3$ ceramics by impedance spectroscopy and Raman study ", *Phase Transitions*, **86**, 703-714 (2013).

[18] C. Ang, Z. Jing and Z. Yu," Ferroelectric relaxor $Ba(Ti,Ce)O_3$", *J. Phys.: Condens. Matter*, **14**, 8901 (2002).

[19] K. Brajesh, A. K. Kalyani and R. Ranjan," Ferroelectric instabilities and enhanced piezoelectric response in Ce modified $BaTiO_3$ lead-free ceramics ",*Appl. Phys. Lett.*, **106**, 012907. 17 (2015).

[20] A. Chen, Y. Zhi, J. Zhi, P. Vilarinho and J. Baptista," Synthesis and characterization of $Ba(Ti_{1-x}Ce_x)O_3$ ceramics ", *J. Eur. Ceram. Soc.*, **17**, 1217-1221 (1997).

[21] L.-F. Zhu, B.-P. Zhang, L. Zhao and J.-F. Li," High piezoelectricity of $BaTiO_3$–$CaTiO_3$–$BaSnO_3$ lead-free ceramics ", *J. Mater. Chem. C*, **2**, 4764-4771 (2014).

[22] H. Du, W. Zhou, F. Luo, D. Zhu, S. Qu and Z. Pei," Phase structure, dielectric properties, and relaxor behavior of $(K_{0.5}Na_{0.5})NbO_3$–$(Ba_{0.5}Sr_{0.5})TiO_3(K_{0.5}Na_{0.5})NbO_3$–$(Ba_{0.5}Sr_{0.5})TiO_3$ lead-free solid solution for high temperature applications ", *J. Appl. Phys.*,**105**, 124104 (2009).
[23] J. P. Praveen, K. Kumar, A. James, T. Karthik, S. Asthana and D. Das," Large piezoelectric strain observed in sol–gel derived BZT–BCT ceramics ", *Curr. Appl. Phys.*, **14**, 396-402 (2014).
[24] S. Patel, A. Chauhan, S. Kundu, N. A. Madhar, B. Ilahi, R. Vaish and K. Varma," Tuning of dielectric, pyroelectric and ferroelectric properties of $0.715Bi_{0.5}Na_{0.5}TiO_3$-$0.065BaTiO_3$-$0.22SrTiO_3$ ceramic by internal clamping", *AIP Adv.*, **5**, 087145 (2015).
[25] Manish Vaish, M. Sharma, R. Vaish, V.S.Chauhan, "Capacitor and battery charging from hot/cold air usin pyroelectric ceramics" *Integrated Ferroelectrics*. **176,** 160 (2016).
[26] M. Sharma, V.S.Chauhan and R. Vaish, **"**Development of figures of merits for pyroelectric energy harvesting devices" *Energy Tech.* **4**(7), 843 (2016).
[27] Manish Vaish, M. Sharma, R. Vaish, V.S.Chauhan, "Electrical energy generation from hot/cold air using pyroelectric ceramics" *Integrated Ferroelectrics.* **167**(1), 90 (2015)
[28] S. Patel, A. Chauhan and R. Vaish, P. Thomas **"**Enhanced energy storage performance of glass added $0.715Bi_{0.5}Na_{0.5}TiO_3$-$0.065BaTiO_3$-$0.22SrTiO_3$ ferroelectric ceramics" *J. Asian Ceram Soc* **3**, 383 (2015)
[29] Manish Vaish, M. Sharma, R. Vaish, V.S.Chauhan, "Experimental study on waste heat energy harvesting using pyroelectric ceramics" *Energy Tech.* **3**, 768 (2015)

Figure Captions:

[30] Figure 1. X-ray diffraction patterns for $BaCe_xTi_{1-x}O_3$ (BCT) ceramics with compositions x=0, 0.1, 0.12 and 0.15.
[31] Figure 2: SEM images of sintered sample (a) x=0, (b) x=0.1, (c) x=0.12 and (d) x=0.15.
[32] Figure 3.Polarization-electric field (P-E) hysteresis loops of sintered sample at room temperature (303K)and constant electric field of 24kV/cm.
[33] Figure 4. Dielectric constant and dielectric loss (tanδ) for all compositions x=0, 0.1, 0.12 and 0.15.
[34] Figure 5. Curie weiss law for all investigated samples.
[35] Figure 6: Curie temperature as a function of Ce content for all samples.
[36] Figure 7: Piezoelectric constant (d_{33}) for all samples.

Figure 1:

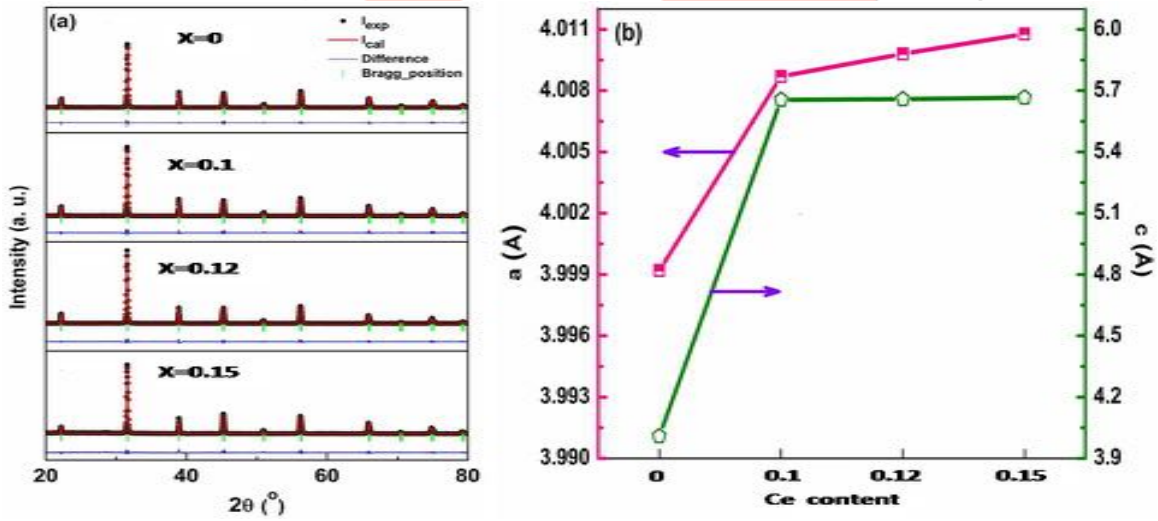

Figure 2:

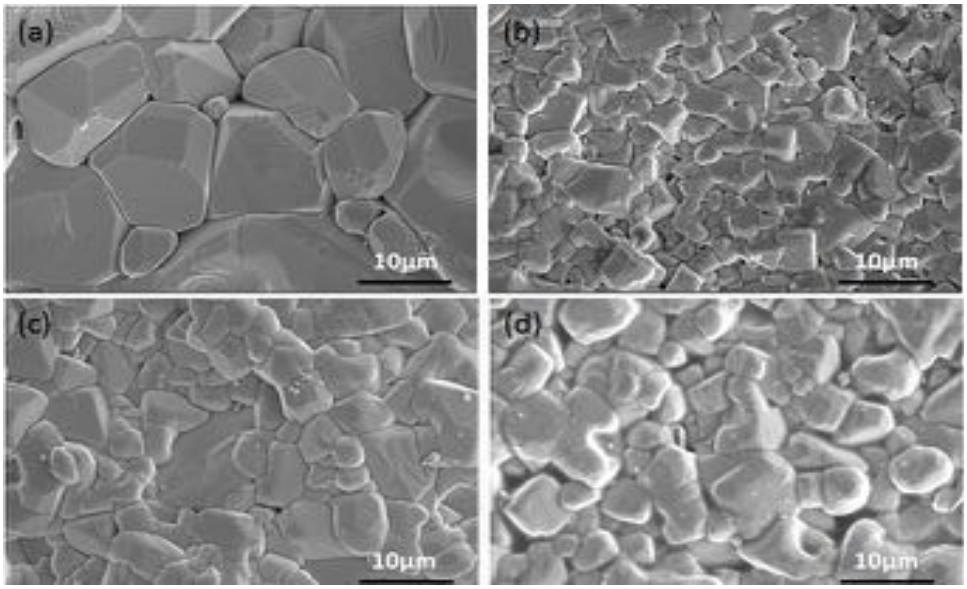

Figure 3:

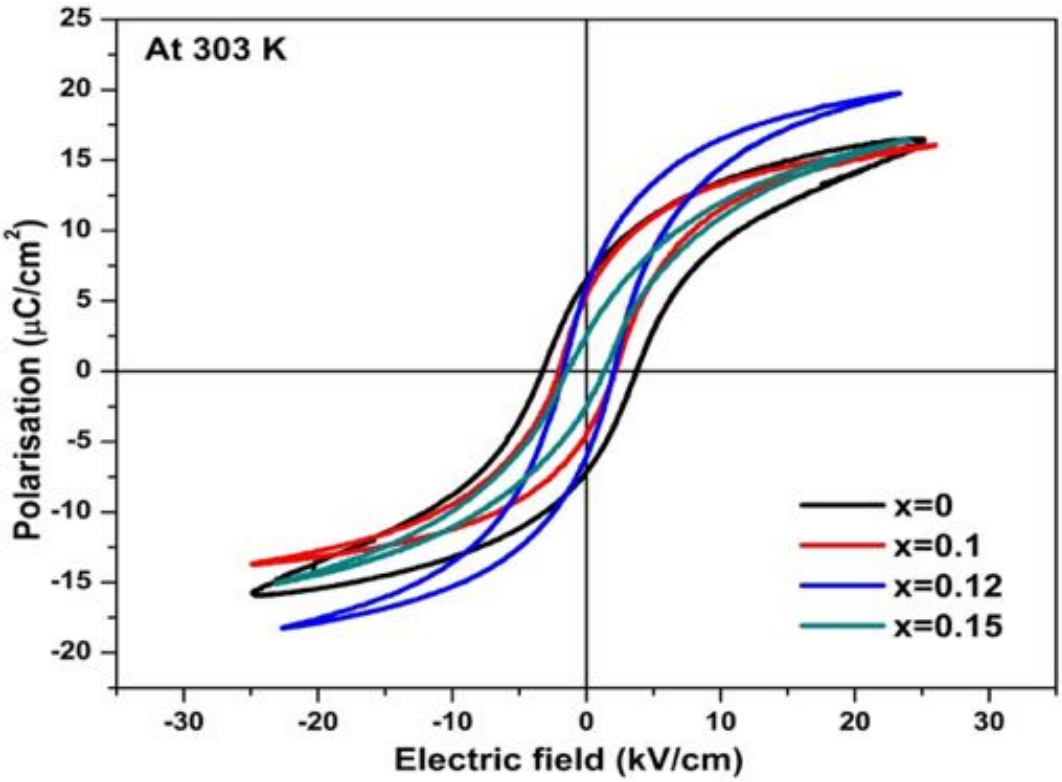

Figure 4:

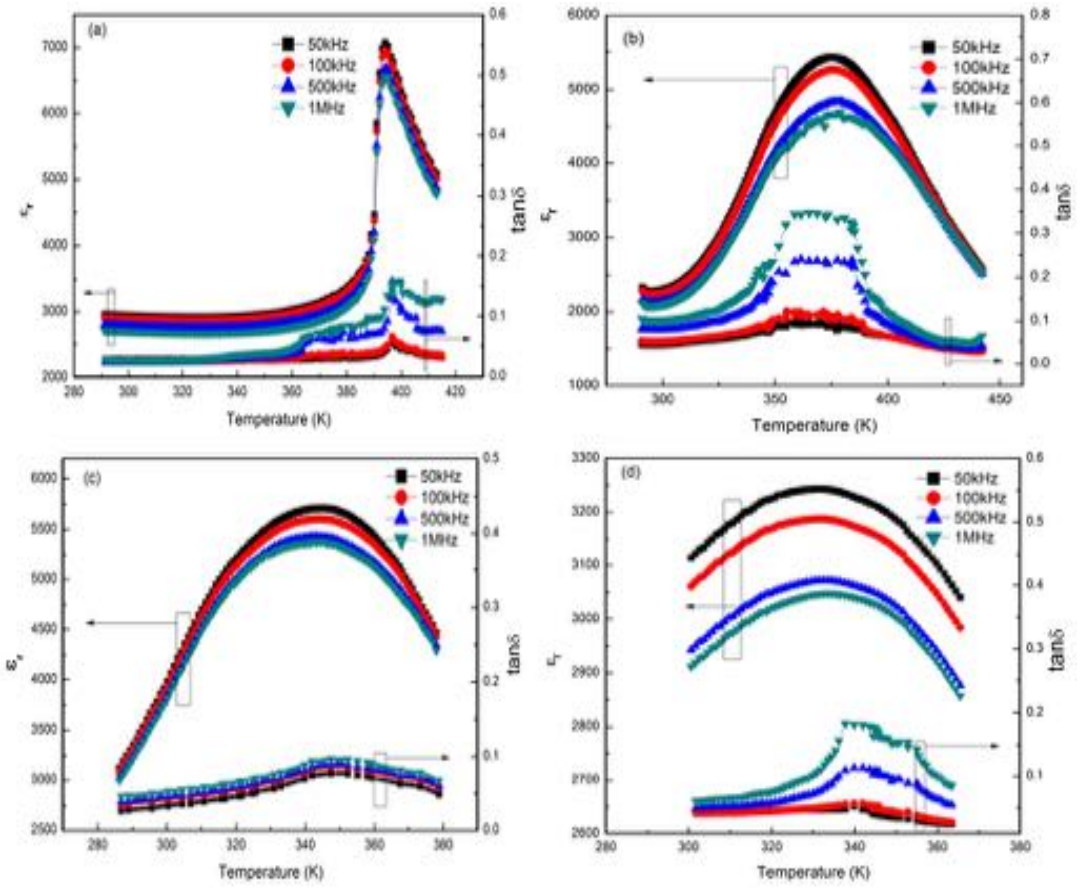
(a)
50kHz
100kHz
500kHz
1MHz
Temperature (K)
(b)
50kHz
100kHz
500kHz
1MHz
Temperature (K)
(c)
50kHz
100kHz
500kHz
1MHz
Temperature (K)
(d)
50kHz
100kHz
500kHz
1MHz
Temperature (K)

Figure 5:

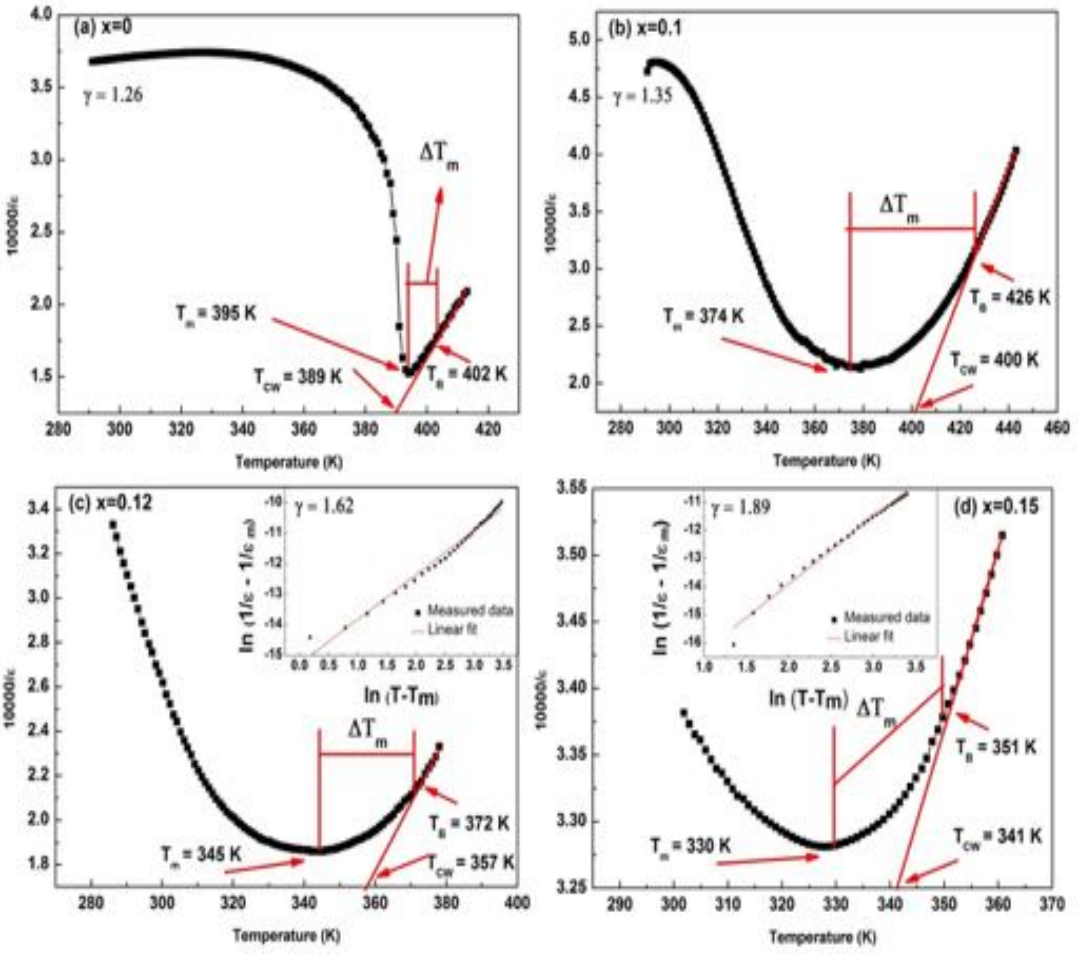
(a) x=0
γ = 1.26
ΔTm
Tm = 395 K
TCW = 389 K
TB = 402 K
Temperature (K)
(b) x=0.1
γ = 1.35
ΔTm
Tm = 374 K
TB = 426 K
TCW = 400 K
Temperature (K)
(c) x=0.12
γ = 1.62
Measured data
Linear fit
ln (T-Tm)
ΔTm
Tm = 345 K
TB = 372 K
TCW = 357 K
Temperature (K)
(d) x=0.15
γ = 1.89
Measured data
Linear fit
ln (T-Tm)
ΔTm
Tm = 330 K
TB = 351 K
TCW = 341 K
Temperature (K)

Figure 6:

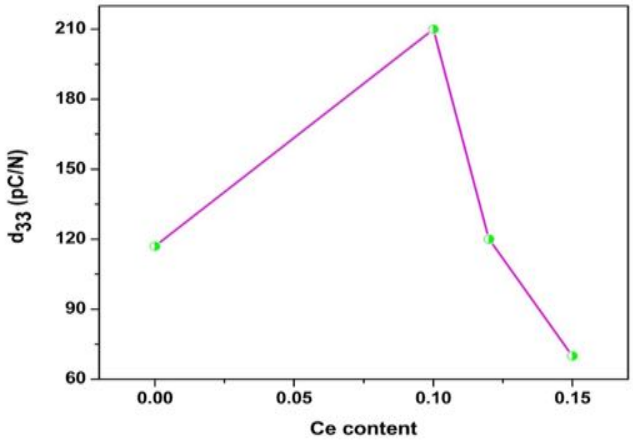

Figure 7: